SUPERRESOLVED WAVE CT AS A PROBLEM OF INVERSE SCATTERING

Toyokatsu MIYASHITA, and Akihiko IWATA
Kyoto Institute of Technology
Department of Electronics and Information Science
Matsugasaki, Sakyo-ku, Kyoto 606 JAPAN

1. INTRODUCTION

Wave CT is an inverse scattering of wave propagation. We constructed the nonlinear basic equations of the wave CT, and solved them. The solution gave superresolved distributions of the wave parameters of the material.

In the reconstructive tomography or CT by microwave or acoustic wave, we must consider the wave properties. We named the problem neatly "Wave CT" insisting on the important role of the wave properties. Mueller et al.[1] developed a method of the inverse problem by Born and Rytov approximations.

We proposed a configuration of the wave CT as shown in Fig.1[2,3]. It belongs to the unbounded field problem. Washisu showed a way to solve such problems combining finite element method (FEM) and boundary element method (BEM) [4]. We proposed a new mathematical approach to the wave CT, after Washisu, combining FEM and BEM[2,3]. We assume that a scalar potential $\phi(r)$ represents the wave field, and that Helmholtz equation of $\phi(r)$ with complex wave number $k(r)$ describes the wave propagation through the material of interest. That is, we describe the wave properties of the material putting the refractive index $n(r)$ and absorption coefficient $\alpha(r)$ into $k(r)$.

We present here computer experiments of wave CT, and its problems.

2. DERIVATION OF BASIC EQUATION OF WAVE CT

We consider a two-dimensional wave CT as shown in Fig.1. A wave source irradiates the object with a monochromatic cylindrical wave. We make a set of measurements of the wave field on a closed curve B rotating the wave source around O, and get the projection data.

We divide the infinite space under investigation into two sub-spaces by the closed curve B. In the internal region S_I. $n(r)$ and $\alpha(r)$ may be inhomogeneous. A homogeneous medium fills the external open space S_0 including the wave source. Then, we make a mathematical formulation after the electromagnetic unbounded field problems by Washisu[4].

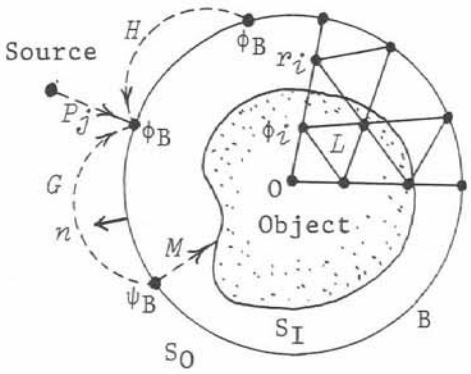

Fig.1. Geometry of "Wave CT" and meaning of variables.

2.1 Internal Closed Region with FEM

We start from the following Helmholtz equation, and use FEM in S_I.

$$\nabla^2\phi(r) + k^2(r)\phi(r) = 0 \quad \text{in } S_I, \text{ with } \partial\phi(r)/\partial n = \psi_B(r) \quad \text{on B.} \tag{1}$$

Here, $k(r) = n(r)k_0 - i\alpha(r)$, and k_0 is the wave number of the free space. Instead of solving the Helmholtz equation directly, we solve it indirectly by calculus of variations using the following functional.

$$I(\phi(r)) = \iint_{S_I}[\{\partial\phi(r)/\partial x\}^2 + \{\partial\phi(r)/\partial y\}^2 - k^2(r)\phi^2(r)]dr - 2\oint_B \phi(r)\psi_B(r)ds. \tag{2}$$

Minimization of the functional by $\phi(r)$ gives both Helmholtz equation and boundary condition (1). We divide the internal region into small triangular elements as shown schematically in Fig.1. Approximating $\phi(r)$ to a linear function of r in each element, we convert the functional (2) into a function of the potential values $\phi(r_i)$'s at the nodes r_i's of the elements. We let the first order variation of the discrete version of the functional (2) for $\phi(r_i)$'s be zero. Then, we obtain an algebraic equation

$$L\Phi = M_B\Psi_B \ . \tag{3}$$

Here L is a matrix which includes $k(r_i)$'s in S_I. The matrix M_B is constant. Φ and Ψ_B are column vectors composed of, respectively, $\phi(r_i)$'s and $\psi_B(r_j)$'s at the nodes r_j's of the boundary elements on B. We approximate also $k^2(r)$ to a linear function of the coordinates in each elements. Then, each element of L becomes a linear function of $k^2(r_i)$'s.

2.2 External Open Space with BEM

We use BEM in S_O, and Helmholtz equation in this space is as follows.

$$\nabla^2\phi(r) + k_0{}^2\phi(r) = -\delta(r_s - r) \qquad \text{in } S_O \tag{4}$$

The right side of eq.(4) represents the wave source. We describe $\phi(r)$ by a boundary integral of $\phi_B(r)$, $\psi_B(r)$ and Green's function of eq.(4). We approximate also $\phi_B(r)$ and $\psi_B(r)$ to linear functions of r. Then, we get an algebraic equation which relates Φ_B and Ψ_B on the boundary B.

$$G\Psi_B = H\Phi_B + P_B \ . \tag{5}$$

Matrices G and H are constant. The vector P_B is also constant, and represents the direct contribution of the wave source to the potential Φ_B.

2.3 Basic Equation of Wave CT by Combination of FEM and BEM

Cutting out Ψ_B from eqs.(3) and (5) gives the basic equation of wave CT.

$$\left[\begin{array}{c|c} L_{II} & L_{IB} \\ \hline L_{BI} & L_{BB} - M_B G^{-1} H \end{array}\right] \left[\begin{array}{c} \Phi_I \\ \hline \Phi_B \end{array}\right] = \left[\begin{array}{c} 0 \\ \hline M_B G^{-1} P_B \end{array}\right] \tag{6}$$

Here, the subscripts I and B show sub-matrices of L or sub-vectors of Φ related to, respectively, the internal nodes and the boundary nodes.

3. PROJECTION DATA

We got here the projection data Φ_B by the eq.(7) derived from eq.(6).

$$\Phi_B = [GM_B{}^{-1}(L_{BB} - L_{BI}L_{II}{}^{-1}L_{IB}) - H]^{-1}P_B \ . \tag{7}$$

We rotated the wave source every 12° around O, and calculated each time Φ_B at 30 nodes on B. Then, we got 30 projection data $\Phi_B{}^s(s = 1,\ldots,S)$, $S = 30$. The radius of B was equal to a wavelength, and the wave source was 1.2 times wavelength apart from O. The total number of nodes including those on the boundary was 91, and the number of the elements was 150.

4. IMAGE RECONSTRUCTION FROM PROJECTION DATA

4.1 Mathematical Method of Image Reconstruction - Nonlinear Optimization

We solve the eq.(6) for $k(r_i)$'s included in L_{II}, L_{IB}, and L_{BI}. The given conditions are the projection data $\Phi_B{}^s$'s. The equations are over-determined and also nonlinear concerning the unknowns $\Phi_I{}^s$ and $k(r_i)$'s. We adopted the

nonlinear optimization method developed by Fletcher and Powell[5]. We considered the function (8) of Φ_I^s's and $k(r_i)$'s as the object function.

$$f(\Phi_I^1, \Phi_I^2, \ldots, \Phi_I^S;\ k(r_1), k(r_2), \ldots)$$

$$= \sum_{s=1}^{S} [\, \| L_{II}\Phi_I^s + L_{IB}\Phi_B^s \|_2 + \| L_{BI}\Phi_I^s + (L_{BB} - M_B G^{-1} H)\Phi_B^s - M_B G^{-1} P_B^s \|_2]. \quad (8)$$

In the iterative minimization of the function, the global feature of the object appeared after about 10 iterations.

4.2 Choice of Initial Value for Nonlinear Optimization and the Result

The wave CT solves nonlinear simultaneous equations, which makes a sharp contrast to other CT's. One of the well-known undesirable properties of nonlinear problems is the dependence of the solution on the initial value of the iteration. We investigated this problem about the wave CT.

Fig.2(a) shows a perspective view of the two-dimensional object. It has two small polygonal targets, whose centers have peak values $\{n(r_2) = 1.3, \alpha(r_2) = 0.3\}$ and $\{n(r_4) = 1.3, \alpha(r_4) = 0.1\}$, buried in a large polygonal medium of $\{n = 1.1, \alpha = 0.1\}$. The small targets have a radius of 0.2 times wavelength, and the large one has a radius of a wavelength. We reconstructed an image from a uniform initial value $\{n = 1.1, \alpha = 0.1\}$. The average error per pel was 0.0095 for $n(r_i)$'s and 0.0100 for $\alpha(r_i)$'s. The precision of the reconstructed local peaks was from 96% to 97%. An image from a uniform value of free space $\{n = 1.0, \alpha = 0.0\}$ had the average errors 0.0088 for $n(r_i)$'s and 0.0105 for $\alpha(r_i)$'s and the precision of the local peaks from 93% to 97%.

Next we show an image from a random value in Fig.2(b). The initial values of $n(r_i)$'s distributed uniformly between 1.0 and 1.2, and $\alpha(r_i)$'s between 0.0 and 0.2. The average error is 0.0095 for $n(r_i)$'s and 0.0086 for $\alpha(r_i)$'s. The precision of the local peaks is from 97% to 98%. These results show not

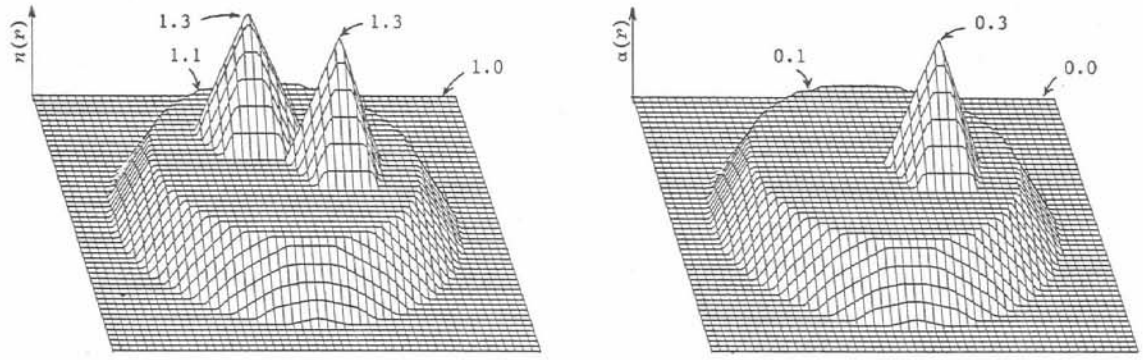

Fig.2. (a)The true image.

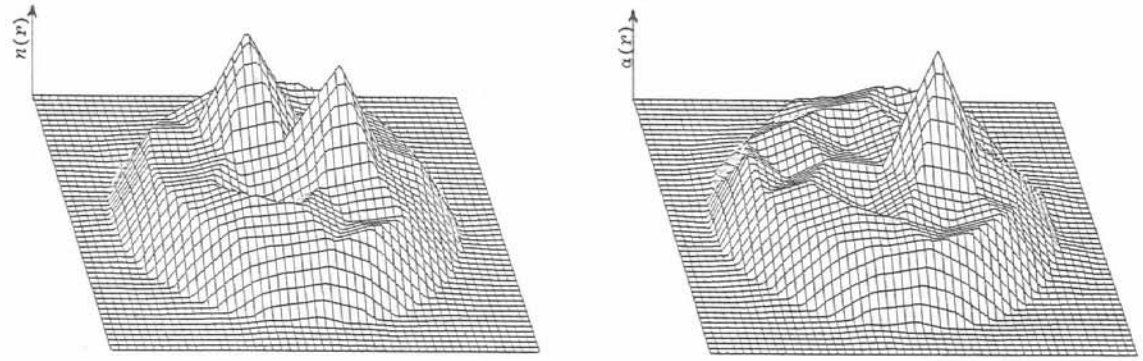

Fig.2. (b)Reconstructed image from random value of $n(r_i) = 1.0$ to 1.2 and $\alpha(r_i) = 0.0$ to 0.2, with 30 iterations.

only the small dependence of the reconstructed images on the initial values, but also the precise reconstruction both in quantity and in quality.

4.3 Dependence of Reconstructed Images on Noise or Error in Projection Data

We investigated degree of image degradation caused by noise or error in the projection data. We show in Fig.3 an image reconstructed from the projection data which has random magnitude error of -30 dB of the average value of the true projection data and random phase error between -1° and +1°. The average error per pel is 0.010 for $n(r_i)$'s and 0.012 for $\alpha(r_i)$'s. The precision of the local peaks is from 93% to 98%. We reconstructed also an image with the random magnitude error of -25 dB and the random phase error between -2° and +2°. The average error was 0.018 for $n(r_i)$'s and 0.012 for $\alpha(r_i)$'s. The precision of the local peaks was from 98% to 100%. Comparing with the above images from the exact projection data, we can say that this degree of noise or error in the projection data is allowable.

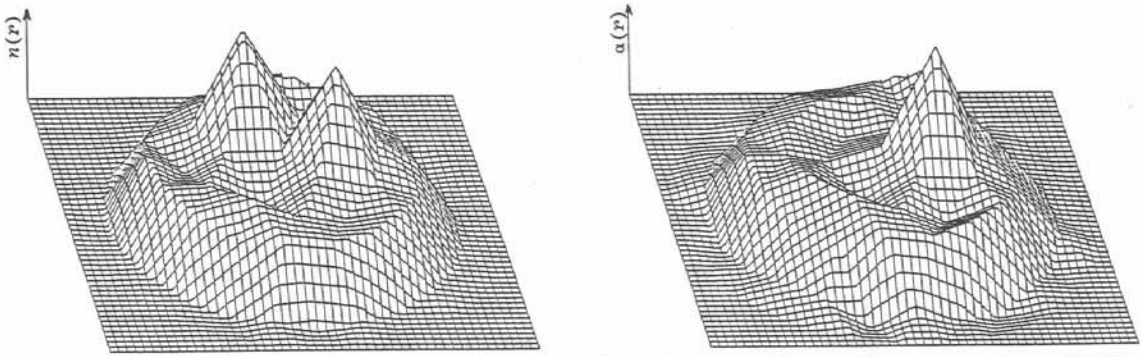

Fig.3. Reconstructed image from projection data with uniform random error of -30 dB in magnitude and between -1° and +1° in phase.

5. CONCLUDING REMARKS

Considering the "Wave CT" as an inverse scattering of wave propagation, we constructed the nonlinear basic equations of the wave CT of closed form. The solution gave superresolved distributions of both refraction index and absorption coefficient of the object simultaneously.

We showed images of small targets and the surrounding uniform medium reconstructed by wave CT with the wave properties of refraction, reflection, diffraction, and attenuation included in the projection data. The precision of reconstruction of the small targets was above 96%, and also the global image was precise both in quantity and in quality. The resolution was better than 0.1 times wavelength. The results showed not only the negligible small dependence of the reconstructed images on the initial values, but also small dependence on the error or the noise included in the projection data.

Precision and capacity of the numerical calculation of the computer determine the limitation of the wave CT.

ACKNOWLEDGMENT

The authors gratefully acknowledge helpful discussions of this problem with Prof. H. Ogura of Kyoto University and Assoc. Prof. J. Nakayama of Kyoto Institute of Technology and former graduate student E. Ueda.

REFERENCES

[1] R.K.Mueller, M.Kaveh and G.Wade: *Proc. IEEE*, 67 p.567, 1979.
[2] E.Ueda and T.Miyashita: *Proc. Technical Group Meeting of IEICE Japan*, EMT-85 p.9, 1985 [in Japanese].
[3] T.Miyashita et al.: *Japan. J. Appl. Phys.*, 27 Suppl.27-1 p.212, 1988.
[4] S.Washisu et al.: *Proc. IECE Japan*, J64-B p.1359, 1981 [in Japanese].
[5] R.Fletcher and M.J.D.Powell: *Comp. J.*, 6, p.163, 1964.